Received July 25, 2019, accepted August 17, 2019, date of publication August 22, 2019, date of current version September 6, 2019.

Digital Object Identifier 10.1109/ACCESS.2019.2936924

Junction Temperature Prediction for LED Luminaires Based on a Subsystem-Separated Thermal Modeling Method

MIAO CAI[1], ZHI LIANG[1], KUN-MIAO TIAN[1], MING-HUI YUN[1], PING ZHANG[1], DAO-GUO YANG[1], AND GUO-QI ZHANG[1,2], (Fellow, IEEE)

[1]School of Mechanical and Electrical Engineering, Guilin University of Electronic Technology, Guilin 541004, China
[2]Delft Institute of Microsystems and Nanoelectronics (Dimes), Delft University of Technology, 2628 CD Delft, The Netherlands

Corresponding authors: Miao Cai (caimiao105@163.com) and Dao-Guo Yang (daoguo_yang@163.com)

This work was supported in part by the National Natural Science Foundation of China under Grant 61865004, in part by the Natural Science Foundation of Guangxi Province under Grant 2018GXNSFAA138033 and Grant 2017GXNSFDA198006, and in part by the Innovation-Driven Development Project of Guangxi Province under Grant AA182420.

ABSTRACT The junction temperature (T_j) of LEDs in an LED luminaire is useful for projecting the luminous flux maintenance or lifetime of luminaires. Normally, a LED luminaire has a unique and complex geometric outline, and its LED package size is only a few millimeters. The thermal modeling procedure with one luminaire model is complex. Achieving a precise T_j of luminaires quickly in modeling is still a great challenge. In this work, aiming at providing a simple modeling method to predict a precise luminaire T_j, a subsystem-separated thermal modeling method for luminaires is proposed by following the existing form of multi-domain modeling. The detailed package model is linked with the luminaire model, while the average temperature at the bottom surface of the LED package is associated with an assumed equivalent convective heat transfer coefficient (ECHTC) at the package model. An adequately assumed ECHTC is obtained, while a unique average temperature is achieved from the luminaire model. Results show that a precise luminaire T_j is projected rapidly by modeling the package model with the adequate ECHTC and a proposed power law equation. The proposed modeling method not only provides a precise T_j prediction with a small error but also effectively simplifies the modeling of LED luminaires.

INDEX TERMS LED luminaires, junction temperature, thermal modeling, prediction, subsystem.

NOMENCLATURE

T_j	Junction temperature (K)
u	Velocity vectors for directions of x (m/s)
v	Velocity vectors for directions of y (m/s)
w	Velocity vectors for directions of z (m/s)
δ	Air density (kg/m^3)
T	Air temperature (°C)
T_Δ	Temperature difference between junction point and solder joint (°C)
k	Thermal conductivity, W/(m×K)
C_p	Heat capacity (J/K)
T_∞	Ambient temperature (°C)
ε	Air kinematic viscosity (m^2/s)
g	Gravitational acceleration (m^2/s)
β	Thermal expansion coefficient (1/°C)
Gr_L	Grashof number
Ra_L	Rayleigh number
T_p	Average temperature at the bottom face of the LED package in package model (°C)
h_a	Assumed ECHTCs W/(m^2×°C)
l	Characteristic length (m)

The associate editor coordinating the review of this article and approving it for publication was Lei Jiao.

I. INTRODUCTION

Light-emitting diodes (LEDs) have triggered a revolution in illumination because of their advantages over traditional light sources, such as high luminous efficiency, energy saving, and long lifetime. However, more than 70% of the input electrical energy is converted into heat in general commercial products. The temperature of the p-n junction, called junction temperature (T_j), is considered a crucial parameter for the reliability of LEDs. The T_j in a LED lamp system, in conjunction with the luminous maintenance database of LED packages

or modules, is useful for projecting the luminous flux maintenance of LED lamps [1]. LED T_j measurement methods can be generally divided into thermal, optical, and electrical measuring methods based on a concrete measured parameter, such as measuring using an embedded micro sensor along LED chip directly [2], determining through a stable linear relationship between T_j and LED light power [3], [4], and a certain T_j relationship to peak wavelength or blue–white ratio of LED devices with self-excited photoluminescence signal [5] or to reverse current in InGaN LEDs [6]. Among the T_j measurement methods, the pulsed T_j measurement (PJTM) is the most appealing method [7], [8]. The PJTM method is based on an evident linear relationship between LED T_j and its associated voltage in a certain range of temperature and the forward current. Uncertainty studies or error comparisons on T_j measurement have recently become a popular topic of discussion [9], [10]. Ye *et al.* [11] proposed an improved pulse-free direct T_j measurement method for HV LEDs to reduce errors and to achieve in situ T_j measurements with DC currents, simple setups, and few step sequences. Further, Chu *et al.* [12] proved that the average T_j of any LED array had a linear relationship with the equivalent impedance, and LED T_j can be determined with the equivalent impedance. However, LED packages or LED modules are generally assembled with a heat sink and an optical structure. Thus, the implementation of the aforementioned T_j measurement approaches for LED lamp systems with a complex geometry structure is impractical [13] unless the system is disassembled.

Thermal modeling can help provide an accurate prediction of the final performance and reliability of a device [14]. Li *et al.* [15] conducted research into LED-integrated light source thermal issues on the principle of heat transfer and proved that LED thermal field analysis based on multiphysics finite element simulation is feasible and effective. Formanek and Jakovenko [16] presented thermal and thermomechanical stimulation for a retrofit LED lamp by using ANSYS and CoventorWare software and by focusing on the thermal modeling of the LED lamp system. The results from different simulation approaches matched well with those from the experiments.

Thermal modeling can effectively analyze the effect of different loading conditions. Jang *et al.* [17] and Shen *et al.* [18] investigated the orientation effect for cylindrical heat sinks and rectangular fin heat sinks under natural convection conditions by using numerical simulation and experiments. Results indicated that dense fin arrays are sensitive to orientation. Schmid *et al.* [19] investigated the effect of a central cylindrical opening on the heat transfer of radial heat sinks for different orientations. This study showed that the opening on the heat sink can greatly improve orientation sensitivity. Costa and Lopes [20] presented a numerical study regarding an improved heat sink for LED lamps that operate under natural convection conditions. Further thermal module designs and analyses on 230 W LED lamps with different incline angles were performed [21]. Ye *et al.* [22] provided an electrical–thermal–luminous–chromatic model to predict light performance with thermal management under in situ temperature. Wang *et al.* [23] developed a thermal model design and conducted an analysis for high-power LED automotive headlight cooling devices. Wang *et al.* [24] presented a thermal design for an LED lamp with air convection. Aiming to enhance heat dissipation and further minimize T_j, researchers conducted numerous studies to fulfill thermal designs by using thermal modeling and analysis [25]–[27].

Modeling analysis on the thermal performance of an LED lamp showed that critical parts can be determined and solutions for thermal problems can be achieved using thermal simulation tools when designing high-power LED lamps [24], [28]–[29]. Yurtseven *et al.* [30] analyzed the temperature distribution of LED luminaires by using a two-resistor compact thermal model. They believed that the use of the two-resistor model and measurement combination is a fast and easy way to predict the thermal behavior of an LED system with acceptable errors. Müller *et al.* [31] further attempted to address several issues with regard to the determination of the junction-to-case thermal resistance for LED packages. On the basis of photo-electro-thermal theory, prediction methods for the thermal effect and optical properties of LED systems were proposed, and the geometrical parameters of the heat sink and optical, electrical, and thermal characteristics of LED systems were linked [32]. Cai *et al.* [1] determined a steady and reliable temperature difference between a junction point and a referenced surface point for an LED lamp and projected the T_j of LED lamps with thermal modeling and surface temperature measurement. The luminous flux maintenance or lifetime of LED packages or lamps can be further projected effectively on the basis of a relationship between LED T_j and lifetime [1], [33].

In general, a real LED luminaire has a unique and complex geometric outline, and various structures are involved in modeling comparison for the design phase of LED luminaires. The LED package size is only a few millimeters, which is considerably smaller than the luminaire dimensions, and meshing and/or modeling procedure for an LED luminaire model with a big and/or complex geometric outline is still a great challenge for a traditional one-model simulation. To solve the combined thermal, electrical and light output simulation problem, Poppe [34], [35] proposed multi-domain compact models of LEDs with an approach that is originally developed for IC chips [36] and created multi-port thermal network models of LED luminaires for application in system-level multi-domain simulation. For a given physical arrangement of an LED luminaire, the effects of variations of the applied LEDs can be analyzed with N subsequent CFD simulations at the lamp system level. Subsequently, multi-domain modeling of LEDs for supporting virtual prototyping of luminaires was presented [37]. However, obtaining a precise T_j of LED luminaires quickly is still a major challenge. The thermal modeling of an LED package without a detailed structure and adequate meshing cannot project an adequate LED T_j accurately. In some cases, this phenomenon results in a great

prediction error on the luminous flux maintenance or lifetime of LED lamps. Existing multi-domain modeling procedures with N subsequent CFD simulations can provide a good solution for analyzing the effects of LED variations at system level, but a fast modeling method for achieving a precise T_j of LED luminaires is still an urgent need. Following the concept of multi-domain modeling [35], [36] and [38], this work aims to provide a simple modeling method to predict a precise luminaire T_j quickly.

In this work, a subsystem-separated thermal modeling method for LED luminaires is proposed to estimate a precise luminaire T_j quickly. First, a thermal model of LED luminaire is established, with its LED package being treated as a uniform heating block. Then, a traditional thermal simulation is conducted at the luminaire level. Second, a detailed isolation model of LED package is established for thermal modeling at the package level. The package model is linked with the luminaire model, while the bottom surface of the LED package is considered a common interface between two isolation models. The average temperature at the bottom surface of the LED package is associated with an assumed equivalent convective heat transfer coefficient (ECHTC) at the package model. An adequately assumed ECHTC is then obtained after a unique average temperature is achieved from the LED luminaire model. A precise lamp T_j is projected by creating a detailed model of an LED package with the adequately assumed ECHTC. In this work, the relationship between the average temperature and the assumed ECHTCs at the package model is investigated.

II. METHODOLOGY

A. THERMAL RESISTANCE DISTRIBUTION IN LED LUMINAIRE

Thermal resistance in a luminaire is complex and is generally distributed in LEDs through packaging material, solder joint, substrate thermal conductor, and heat sink [1]. Evidently, measuring the maximum T_j of LED luminaires directly in a non-destructive manner is infeasible. Thermal modeling can predict the T_j for LED packages and/or luminaires effectively while the junction-to-case thermal resistance is considered [1], [31]. However, the LED package size of only a few millimeters is usually considerably smaller than the luminaire dimensions, and the procedure to ensure a detailed structure and a fine mesh division for LED packages in a luminaire model is time-consuming and difficult. Fig. 1 shows that the thermal resistance of the LED package subsystem can be normally distributed in the LED chip, die-attached layer, package substrate, and LED lens. Thermal modeling of the LED package without a detailed structure and an adequate mesh division cannot project T_j accurately. Moreover, repeating complex meshing and modeling procedure when the LED package is applied on various heat sinks for different design schemes is unavoidable in the design phase. Evidently, the design workload of LED luminaires is heavily based on traditional modeling with a one-luminaire model.

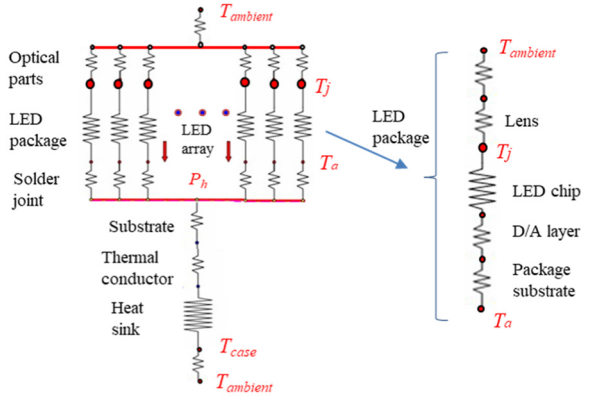

FIGURE 1. Equivalent thermal resistance distribution in LED luminaire [1].

Thermal convection is an important form of heat transfer that occurs at the external surface of LED luminaires that contact with air. Most researchers often neglected the effect of air and specified a constant convection coefficient as a boundary condition during thermal simulation [16], [39]. However, obtaining the convection coefficient accurately is difficult because it varies with different positions in LED luminaires. This work analyzes the heat transfer of solid object within a fluid zone by using computational fluid dynamics (CFD) software.

B. FORMS OF HEAT CONVECTION IN THERMAL MODELING

In general, the mass conservation law, as a basis of physical laws in studying atmospheric motion, can be expressed mathematically using the continuity equation [40] as

$$\frac{\partial}{\partial x}(\delta u)+\frac{\partial}{\partial y}(\delta v)+\frac{\partial}{\partial z}(\delta w)=0 \tag{1}$$

The continuity equation implies that the velocity and density fields for a fluid zone are mutually restrictive around a 3D solid object. Moreover, the momentum equation can be described as [41]

$$u\frac{\partial u}{\partial x}+v\frac{\partial u}{\partial y}+w\frac{\partial u}{\partial z}=-\frac{1}{\rho}\frac{\partial p}{\partial x}+\nu\left(\frac{\partial^2 u}{\partial x^2}+\frac{\partial^2 u}{\partial y^2}+\frac{\partial^2 u}{\partial z^2}\right) \tag{2-1}$$

$$u\frac{\partial v}{\partial x}+v\frac{\partial v}{\partial y}+w\frac{\partial v}{\partial z}=-\frac{1}{\rho}\frac{\partial p}{\partial x}+\nu\left(\frac{\partial^2 v}{\partial x^2}+\frac{\partial^2 v}{\partial y^2}+\frac{\partial^2 v}{\partial z^2}\right)+g\beta(T-T_\infty) \tag{2-2}$$

$$u\frac{\partial w}{\partial x}+v\frac{\partial w}{\partial y}+w\frac{\partial w}{\partial z}=-\frac{1}{\rho}\frac{\partial p}{\partial x}+\nu\left(\frac{\partial^2 u}{\partial x^2}+\frac{\partial^2 u}{\partial y^2}+\frac{\partial^2 u}{\partial z^2}\right) \tag{2-3}$$

In addition, the energy equation for a 3D heating solid object in the fluid zone can be described as [40]

$$\mathrm{u}\frac{\partial \mathrm{w}}{\partial \mathrm{x}}+\mathrm{v}\frac{\partial \mathrm{w}}{\partial \mathrm{y}}+\mathrm{w}\frac{\partial \mathrm{w}}{\partial \mathrm{z}}=-\frac{1}{\rho}\frac{\partial \mathrm{p}}{\partial \mathrm{x}}+\mathrm{v}\left(\frac{\partial^2 \mathrm{u}}{\partial \mathrm{x}^2}+\frac{\partial^2 \mathrm{u}}{\partial \mathrm{y}^2}+\frac{\partial^2 \mathrm{u}}{\partial \mathrm{z}^2}\right) \tag{3}$$

and the air flow can be normally expressed as follows [41]:

$$u\frac{\partial T}{\partial x}+v\frac{\partial T}{\partial y}+w\frac{\partial T}{\partial z}=\alpha\left(\frac{\partial^2 T}{\partial x^2}+\frac{\partial^2 T}{\partial y^2}+\frac{\partial^2 T}{\partial z^2}\right) \quad (4)$$

where u, v, and w are the velocity vectors for directions x, y, and z, respectively; δ is the air density; T is the fluid temperature. T_∞ is the ambient temperature; C_p and k are the specific heat capacity and thermal conductivity of the object at constant pressure, respectively; g is the gravitational acceleration; β is the thermal expansion coefficient; and α is the thermal diffusivity. A natural convection matter is usually described using the Grashof number to describe the flowing status of hot air [41] as follows:

$$Gr_L=\frac{gl^3\beta\left(T_j-T_\infty\right)}{\varepsilon^2} \quad (5)$$

where l is the characteristic length or/and diameter for a specified heat sink; ε is the air kinematic viscosity; and β is the thermal expansion coefficient. In general, natural convection can be divided into two forms, namely, laminar and turbulent flows, by using Rayleigh number (RaL) [42] as follows:

$$Ra_L=Gr_L\times P_r=\frac{gl^3\beta\left(T_j-T_\infty\right)}{\varepsilon\alpha} \quad (6)$$

where P_r is the Prandtl number, and $P_r=\varepsilon/\alpha$. For the external flow of an LED luminaire, the natural convection form can be regarded as laminar flow when $10^{-6}\leq Ra_L<10^9$ and as turbulent flow when $Ra_L\geq 10^9$.

C. SUBSYSTEM-SEPARATED THERMAL MODELING APPROACH AND JUNCTION TEMPERATURE PROJECTION

First, a thermal model of an LED luminaire is established, and its LED package is treated as a uniform heating block to simplify the meshing and/or modeling procedure. The traditional thermal simulation is subsequently conducted within a fluid zone by using CFD software at the luminaire level. The R_{aL} for two luminaires investigated in this work is approximately 2.95×10^9. Thus, the thermal modeling is set up in turbulent flow form. Second, an LED package model with its detailed structure and a fine mesh division is established for thermal modeling at the package level. The R_{aL} for two types of packages analyzed in this work is approximately 2.84×10^2. Therefore, the laminar flow form should be considered in thermal modeling. Various assumed ECHTCs are loaded on the bottom face of the LED package at the package model, and a correlation function between the assumed ECHTCs (h_a) and the average temperature (T_p) at the bottom face of the LED package can be achieved. According to the result of this work, a power law equation is proposed as the correlation function, namely,

$$T_p=f\left(h_a\right)=\rho*h_a^{-\gamma} \quad (7)$$

where γ and ρ are the fitting parameters. As the LED heat power increases, the parameter power (γ) increases in a positive power law and trends to a stable value of approximately 1. Specifically, when $\gamma=1$, ρ is close to the heat flux or/and heat power density of the LED package.

Normally, the temperature distribution of an LED package varies among different LED packages on the LED module of luminaire. The LED package with the highest temperature should be regarded as the critical package of the luminaire. A unique average temperature (T_a) at the bottom face of the critical package can be obtained from the thermal modeling of the luminaire model. Considering an LED package modeling with a real thermal condition at the lamp level, Equation (7) would be revised as follows:

$$h_a=f^{-1}\left(T_p\right)=f^{-1}\left(T_a\right) \quad (8)$$

Then, a proper h_a for an LED package model considered as the real thermal condition at the lamp level can be achieved. In this work, a precise luminaire T_j is expected to be estimated after the obtained proper h_a is applied to the package model. The schematic of the modeling method is shown in Fig. 2.

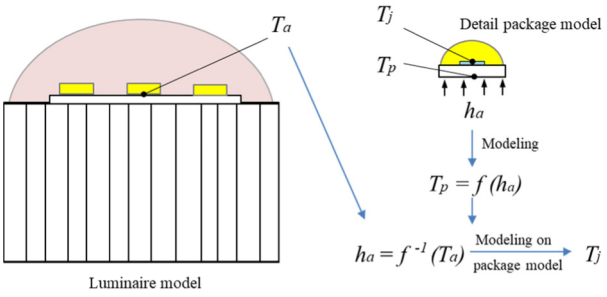

FIGURE 2. Schematic of package isolation modeling method.

In this work, two commercial LED indoor luminaires, which are the most popular forms of indoor LED applications, are considered as the analysis objective (Fig. 3). These luminaires are 13 W LED downlight (Lamp A) with 36 0.32 W horizontal-chip InGaN/GaN LED packages (Package I) in series and 12 W LED spotlights (Lamp B) with 6 1.7 W flip-chip InGaN/GaN LED packages (Package II) in series. Lamp B is composed of an LED module, a driver, an optical part, a compact heat sink, and a fixture. The driver in Lamp B is located inside the luminaire and operates under 220 V input voltage and a constant output current. The driver in Lamp A is independent from other parts. Following the concept of multi-domain modeling [35], [38], two isolated models are established with the ANSYS Icepak simulation tool for the LED luminaire and package in advance. The LED packages are treated as heating blocks in luminaire-level models (Fig. 3), and the geometry structures of the LED packages without bonding wire are described in detail in the package-level models (Fig. 4). The material properties of Lamp A and package are listed in Table 1. The LED heating power of 0.24 and 1.27 W is loaded in the thermal modeling for Packages I and II, respectively. The self-heating of phosphor power is not considered for modeling in this work.

The Icepak solver can automatically simulate the natural convection flow field based on a Boussinesq hypothesis.

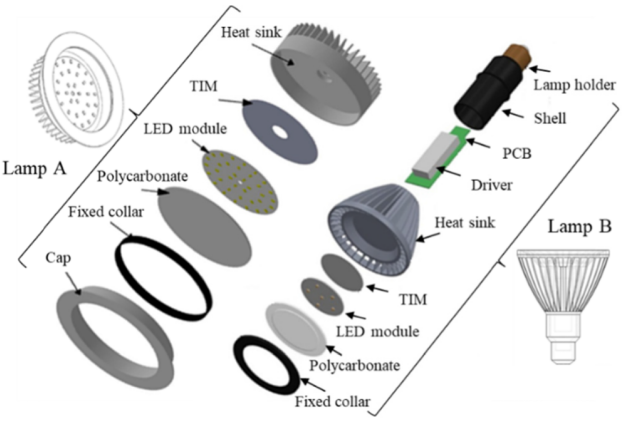

FIGURE 3. Schematic of LED luminaire models.

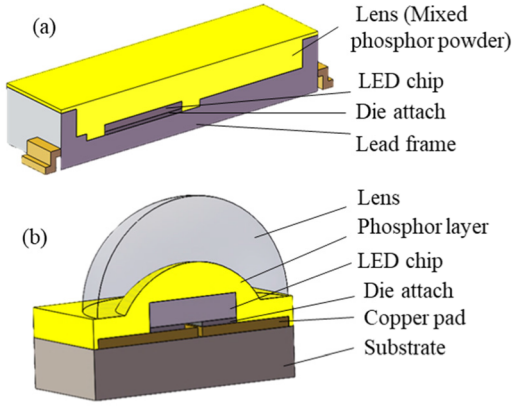

FIGURE 4. LED packages I (a) and II (b) structures for lamps A and B.

TABLE 1. Material properties of lamps A and B and packages I and II for thermal modeling.

Materials	Thermal conductivity, W/(m·K)	Materials	Thermal conductivity, W/(m·K)
Al duralumin (heat sink)	164	Plastic for Shell	0.5
Thermal interface material (TIM)	1.5	Plastic for Fixed Collar	0.5
Substrate of LED module (X/Y/Z)	78/78/2.5	GaN for LED chip	130
Lead Frame	0.8	Die attach	2.5
Polycarbonate	0.23	Al_2O_3 for Substrate	27.2
FR4 for PCB (X/Y/Z)	27/27/0.35	Epoxy resin for Lens	0.2
Al alloy for Cap	100	Phosphor	15
Driver	4	Copper	130

Following the principle of the Icepak solver, when the maximum feature size of a 3D model is defined as L, the distance to the model surface in the Y-axis positive direction and Y-axis gravity direction should be 2L and L, respectively. Accordingly, the distance to the model surface in the other four directions should be 0.5 L. Therefore, one adequate cuboid air zone for each selected lamp model is built as a computational domain in Icepak. The boundaries of the cuboid zone are open to allow airflow. The thermal modeling of the luminaire-level model is set up in a turbulent flow form. The environmental temperature is 25 °C under standard atmospheric pressure, and gravity, which is critical for natural convection, is specified at 9.8 m/s^2 in the z-direction. By contrast, one cuboid air zone with the same size as the package outline is built as a computational domain for each package-level model. Most of the heat generated by the LED chip during operation is assumed to be emitted from the bottom of the package. The laminar flow form is applied in the thermal modeling of the package-level model. The assumed ECHTC is loaded on the bottom surface of the package model.

Moreover, the cumulative structure functions are experimentally measured by the T3Ster tester [43], and the thermal resistance between the junction point and solder joint of the LED package can be observed based on the cumulative structure functions [44]. The experimental luminaire T_j is obtained by [7]

$$T_j = T_R + T_\Delta = T_R + P_h * R_{th} \tag{9}$$

where T_R is the temperature of the solder joint of the LED package, and measured with a thermal couple; T_Δ is the temperature difference between the junction point and the solder joint; P_h is the heating power of the LED package; and R_{th} is the thermal resistance change from T_j to T_p. In this work, comparisons of the temperature distributions of luminaries and packages and the effects of assumed ECHTC on T_p are investigated. Moreover, errors of projected T_j are performed. In consideration of the possible errors from the deviation of testers ($\leq 2\%$) and additional deviation from the testing process ($\leq 2\%$), the confidence level of all experimentally derived data should be approximately 95% in this study.

III. RESULTS AND DISCUSSION

A. THERMAL MODELING ON LED LUMINAIRES

Fig. 5 shows the temperature distributions for Lamp A in the cuboid air zone, including three conditions that consider the effect of luminaire optical parts with/without thermal

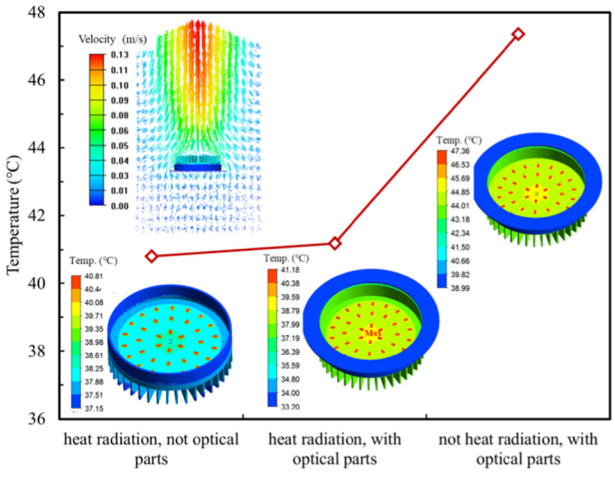

FIGURE 5. Thermal modeling results of Lamp A under various modeling conditions.

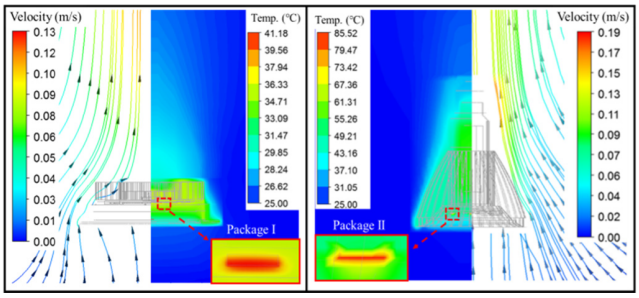

FIGURE 6. Temperature contours and velocity streamlines for Lamps A (left) and B (right).

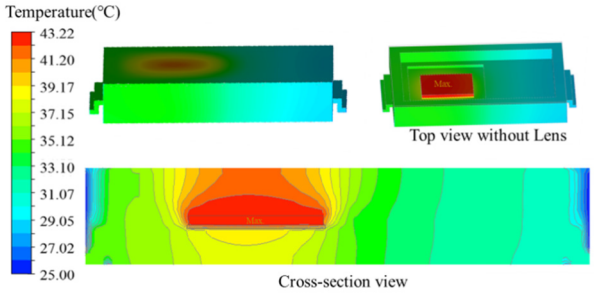

FIGURE 7. Temperature distribution of LED Package I in the package-level model.

radiation boundary condition and ignoring the luminaire optical parts without loading thermal radiation boundary. Evidently, the T_j of the LED luminaire is greatly affected by the thermal radiation and optical parts. The luminaire temperature distribution may reduce by 5 °C–10 °C when the optical cover is removed [45]. Thermal modeling would overestimate the heat dissipation efficiency of LED luminaires when the heat sink without the heat radiation or/and optical parts is considered. Therefore, thermal modeling in the cuboid air zone for LED luminaires should consider the effects of the thermal radiation boundary and the optical parts.

Considering the effects of thermal radiation and optical parts, the luminaire thermal modeling, temperature contours, and velocity streamlines in the cross view for Lamps A and B are achieved, as shown in Fig. 6. Notably, the heat sink of Lamp B is considerably smaller than that of Lamp A; thus, the temperature of Lamp B is considerably higher than that of Lamp A, although the surface cool air flow of Lamp B is stronger than that of Lamp A. In the two cases, the cool air that flows from the bottom and the sides is attracted by the hot heat sink of the LED luminaires. This air is subsequently warmed when it passes through the fin arrays and rises upward in a chimney-like pattern, as shown in the inserted velocity distribution for each luminaire in Fig. 5. Correspondingly, a temperature contour for LED luminaire that approaches a real situation can be obtained.

B. RELATIONSHIP BETWEEN h_a AND T_p IN SEPARATED LED PACKAGE MODELS

Different assumed ECHTCs are loaded to the bottom surface of the LED packages in the package models, including

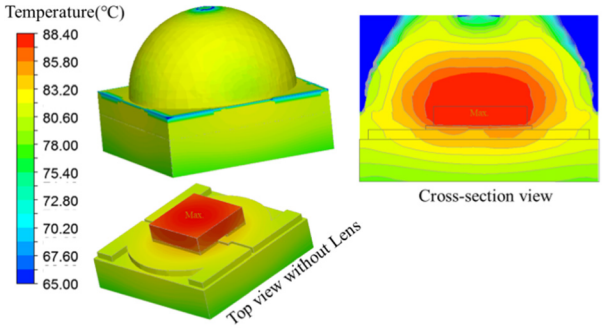

FIGURE 8. Temperature distribution of LED Package II in the package-level model.

Packages I and II. The separate thermal modeling of LED packages is complemented. The detailed temperature distributions for Packages I (Fig. 7) and II (Fig. 8) are provided. Evidently, the temperature contours from the separated package models in the laminar flow form of natural convection can be presented in detail. Meanwhile, a series of average temperature at the bottom face of the LED package is achieved for each package (Fig. 9). The results show that power law function with a negative power (γ) is a good candidate to fit the relationship between the assumed ECHTCs (h_a) and the average temperature (T_p) for the two packages. The power function is $T_p = 215.97{*}h_a^{-0.227}$ and $T_p = 16728{*}h_a{}^{-0.64}$ for Packages I and II, respectively. Notably, the h_a for high-power Package II shows a remarkable impact on T_p. By contrast, h_a for mid-power Package I affects T_p slightly. A large heat power density corresponds to the great effect of h_a on the temperature distribution of the LED package.

Different LED heat powers in 13 levels from 0.5 W to 5 W are loaded to the Package II model to illustrate the effect of LED heat power on the achieved power law function ($T_p = \rho{*}h_a^{-\gamma}$, namely, Equation [7]), as shown in Fig. 10. Evidently, as the LED heat power increases, all parameters of the power law function increase. The heat power density shows an evident effect on the fitting parameters of the power function. The parameter power (γ) increases in a positive power law and trends to a stable value of approximately 1. Specifically, when $\gamma = 1$, the achieved power law function becomes $\rho = T_p{*}h_a$, thereby implying that as the LED heat power increases, the parameter ρ would be close to the heat flux or/and heat power density of the LED package while the unit (W/m^2) of $T_p{*}h_a$ result is considered.

C. T_j PROJECTION AND VALIDATION FOR LED LUMINAIRES

On basis of the luminaire-level modeling, a unique maximum average temperature (T_a) of 40.46 and 80.27 °C at the bottom faces of the LED package (which is treated as a heating block) for Lamps A and B, respectively, can be obtained. On the basis of the power law functions obtained from luminaire-level modeling, namely, $T_p = 215.97{*}h_a^{-0.227}$

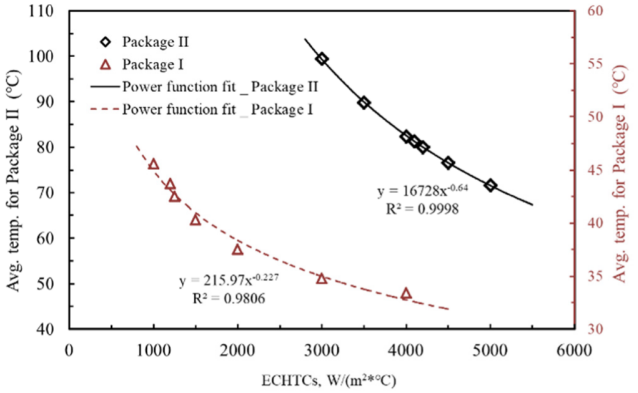

FIGURE 9. Relationship between h_a and T_p in the package models.

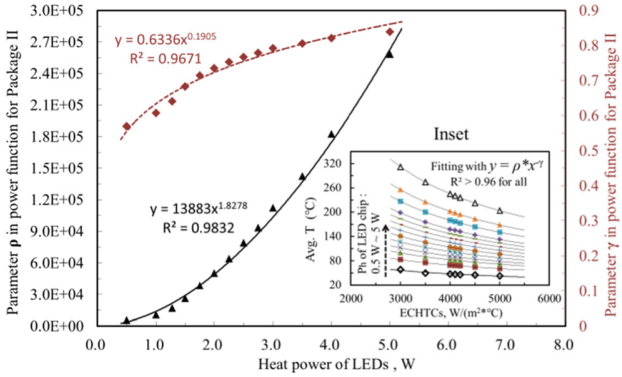

FIGURE 10. Parameter trends with different LED heat powers in the power law function for Package II (Inset: Relationship between ha and Tp for Package II in the package model).

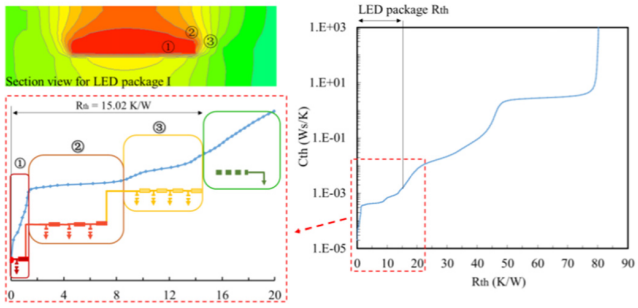

FIGURE 11. Cumulative structure functions and 3D thermal resistance distribution for Lamp A.

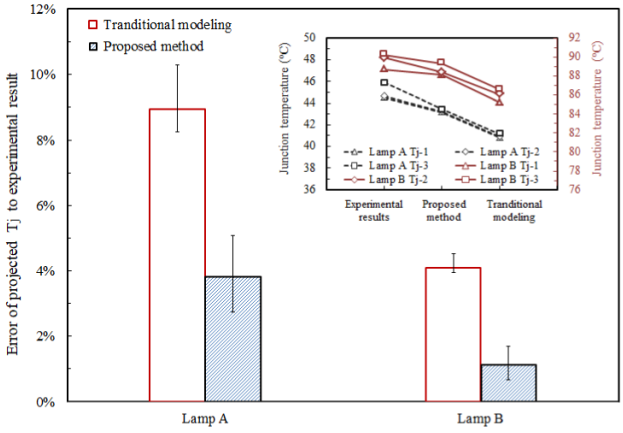

FIGURE 12. Errors of estimated T_j for Lamps A and B through a comparison with the experimental results (Inset: T_j results summarized for three situations).

and $T_p = 16728^* h_a^{-0.64}$ for Packages I and II, respectively, a properly assumed ECHTC (h_a) for the LED package modeling that is considered a thermal condition in the lamp level is achieved with Equation (8). Then, the proper h_a for the package model is obtained as 1600 $W/(m^2 \times^\circ C)$ and 4200 $W/(m^2 \times^\circ C)$ for Packages I and II, respectively. The properly assumed ECHTCs are loaded to the bottom surface of the LED packages in the package models, and the thermal modeling of LED packages is complemented. The temperature distributions with detailed temperature contours for Packages I (Fig. 7) and II (Fig. 8) are given. In the cross-section view, a thermal resistance distribution of LED package can be clearly elucidated based on a cumulative structure function measured experimentally by the T3Ster tester [43], [44]. The thermal resistance distribution of Package I is shown in Fig. 11. From a 3D perspective, temperature contour zones 1, 2, and 3 should form the thermal resistances of the LED chip, the die-attached layer, and the package substrate, respectively. The thermal resistance of the LED package for Lamp A should be approximately 15 K/W (19.2 K/W for Lamp B).

According to the change in thermal resistance observed from cumulative structure functions, T_j can be calculated using Equation (9) [7]. Three LED T_j results from the experimental measurement, proposed modeling, and traditional modeling are summarized for each luminaire (Fig. 12). Fig. 12 shows that the T_j results of the proposed method are close to those of the experimental measurement. The average error of the proposed modeling for Lamp A is 3.82% (approximately 1.12% for Lamp B) more precise than that of traditional simulations (approximately 8.95% and 4.10% for Lamps A and B, respectively). Evidently, when the proposed subsystem-separated modeling method is adopted, the precise prediction improvement of luminaire T_j is more than doubled, and the improvement on Lamp B with a compact heat sink is more obvious than that on Lamp A with a big heat sink. The lamp heat sink volume and/or lamp heat dissipation capacity may be one of the key factors that affect the thermal modeling errors because of the impact of meshing and/or modeling procedure in the luminaire-level model.

In short, the proposed modeling method should involve three steps: (1) the luminaire model is modeled with the LED package treated as a uniform heating block, and T_a is obtained; (2) the package model is initially modeled with various assumed ECHTCs (h_a) and a function $T_p = f(h_a)$, namely, the power law function $T_p = \rho^* h_a^{-\gamma}$, is obtained, and then a proper assumed ECHTC is obtained based on

$T_a = T_p = f(h_a)$; and (3) the package model is modeled again with the proper assumed ECHTC, and then the T_j of the LED luminaires (namely, maximum T_j of the luminaire) can be achieved. The application of the assumed ECHTC is crucial in the three-step modeling procedure. The detailed package model is linked with the luminaire model, while the average temperature at the bottom surface of the LED package is associated with the assumed ECHTC at the package model. Following the previous work [1], the goal of this work is to obtain a precise maximum T_j of LED luminaires quickly and then access its lifetime feature. Evidently, the proposed modeling method for LED luminaires can quickly achieve precise prediction and considerably simplify the meshing and modeling procedure of LED luminaires, especially for luminaires with big and/or complex structures. The method is crucial for fast T_j prediction and/or lifetime assessment of LED luminaires.

IV. CONCLUSION

In this work, a subsystem-separated modeling method for LED luminaires is proposed to estimate a precise luminaire T_j. Two types of commercial LED luminaires are involved in the investigation. The result indicates that assuming ECHTCs at the bottom face of the LED package for the package model is a feasible approach to fulfill the subsystem-separated modeling procedure. A great heat power density corresponds to a substantial effect of the assumed ECHTCs on the temperature distribution of the LED package. The power law function with a negative power is a potential candidate to present the relationship between the assumed ECHTCs and the average temperature at the bottom face of the LED package. The precise prediction improvement of the luminaire T_j with the use of the proposed modeling method is more than double that obtained by the traditional one-model simulation. The improvement of Lamp B with a compact heat sink is more obvious than that of Lamp A with a big heat sink. The lamp heat sink volume and/or lamp heat dissipation capacity may be one of the key factors that affect the errors of lamp thermal modeling. In addition, the temperature contours in the separated package model can present the thermal resistance distribution of the LED package well based on an experimental cumulative structure function. Evidently, the proposed modeling method for LED luminaires can effectively provide precise prediction with a small error and remarkably simplify the meshing and modeling procedure of LED luminaires. The proposed subsystem-separated modeling method is expected to be significant for the rapid reliability assessment of LED luminaires.

REFERENCES

[1] M. Cai, D. Yang, K. Tian, W. Chen, X. Chen, P. Zhang, X. Fan, and G. Zhang, "A hybrid prediction method on luminous flux maintenance of high-power LED lamps," *Appl. Therm. Eng.*, vol. 95, pp. 482–490, Feb. 2016.

[2] C.-Y. Lee, A. Su, Y.-C. Liu, W.-Y. Fan, and W.-J. Hsieh, "*In situ* measurement of the junction temperature of light emitting diodes using a flexible micro temperature sensor," *Sensors*, vol. 9, no. 7, pp. 5068–5075, Jul. 2009.

[3] B. Siegal, "Practical considerations in high power LED junction temperature measurements," in *Proc. 31st IEEE/CPMT Int. Electron. Manuf. Technol. Symp. (IEMT)*, Petaling Jaya, Malaysia, Nov. 2007, pp. 62–66.

[4] E. M. Sa, F. L. M. Antunes, and A. J. Perin, "Junction temperature estimation for high power light-emitting diodes," in *Proc. IEEE Int. Symp. Ind. Electron.*, Vigo, Spain, Jun. 2007, pp. 3030–3035.

[5] N. C. Chen, Y. N. Wang, C. Y. Tseng, and Y. K. Yang, "Determination of junction temperature in AlGaInP/GaAs light emitting diodes by self-excited photoluminescence signal," *Appl. Phys. Lett*, vol. 89, no. 10, Sep. 2006, Art. no. 101114.

[6] B. Wu, S. Lin, T.-M. Shih, Y. Gao, Y. Lu, L. Zhu, G. Chen, and Z. Chen, "Junction-temperature determination in InGaN light-emitting diodes using reverse current method," *IEEE Trans. Electron Devices*, vol. 60, no. 1, pp. 241–245, Jan. 2013.

[7] A. Keppens, W. R. Ryckaert, G. Deconinck, and P. Hanselaer, "High power light-emitting diode junction temperature determination from current-voltage characteristics," *J. Appl. Phys*, vol. 60, no. 9, Nov. 2008, Art. no. 093104.

[8] H.-C. Cheng, J.-Y. Lin, and W.-H. Chen, "On the thermal characterization of an RGB LED-based white light module," *Appl. Therm. Eng.*, vol. 38, pp. 105–116, May 2012.

[9] X. Fu and X. B. Luo, "Can thermocouple measure surface temperature of light emitting diode module accurately?" *Int. J. Heat Mass Transf.*, vol. 65, pp. 199–202, Oct. 2013.

[10] A. Jayawardena, Y.-W. Liu, and N. Narendran, "Analysis of three different junction temperature estimation methods for AC LEDs," *Solid-State Electron.*, vol. 86, pp. 11–16, Aug. 2013.

[11] H. Ye, X. Chen, H. van Zeijl, A. W. J. Gielen, and G. Zhang, "Thermal transient effect and improved junction temperature measurement method in high-voltage light-emitting diodes," *IEEE Electron Device Lett.*, vol. 34, no. 9, pp. 1172–1174, Sep. 2013.

[12] J. Chu, F. Rao, and J. Gguo, "Equivalent impedance method for determining the junction temperature of LED array," *Mod. Phys. Lett. B*, vol. 31, nos. 19–21, Jun. 2017, Art. no. 1740021.

[13] M. Cai, D. G. Yang, S. Koh, C. A. Yuan, W. B. Chen, B. Y. Wu, and G. Q. Zhang, "Accelerated testing method of LED luminaries," in *Proc. EuroSimE*, Cascais, Portugal, Apr. 2012, pp. 1/6–6/6.

[14] Department of Energy (DOE), Washington, DC, USA. *Solid State Lighting Research and Development: Manufacturing Roadmap*. Accessed: Jul. 2011. [Online]. Available: http://apps1.eere.energy.gov/buildings/publications/pdfs/ssl/ssl_mfg_roadmap_aug2014.pdf

[15] J. Li, Q. Yang, P. Niu, L. Jin, B. Meng, Y. Li, Z. Xiao, and X. Zhang, "Analysis of thermal field on integrated LED light source based on COMSOL multi-physics finite element simulation," *Phys. Procedia*, vol. 22, pp. 150–156, Dec. 2011.

[16] J. Formanek and J. Jakovenko, "Thermal characterization and lifetime prediction of LED boards for SSL lamp," *Radioengineering*, vol. 22, no. 1, pp. 245–250, Apr. 2013.

[17] D. Jang, S.-J. Park, S.-J. Yook, and K.-S. Lee, "The orientation effect for cylindrical heat sinks with application to LED light bulbs," *Int. J. Heat Mass Transf.*, vol. 71, pp. 496–502, Apr. 2014.

[18] Q. Shen, D. Sun, Y. Xu, T. Jin, and X. Zhao, "Orientation effects on natural convection heat dissipation of rectangular fin heat sinks mounted on LEDs," *Int. J. Heat Mass Transf.*, vol. 75, pp. 462–469, Aug. 2014.

[19] G. Schmid, L. Valladares-Rendón, T.-H. Yang, and S.-L. Chen, "Numerical analysis of the effect of a central cylindrical opening on the heat transfer of radial heat sinks for different orientations," *Appl. Therm. Eng.*, vol. 125, pp. 575–583, Oct. 2017.

[20] V. A. F. Costa and A. M. G. Lopes, "Improved radial heat sink for LED lamp cooling," *Appl. Therm. Eng.*, vol. 70, no. 1, pp. 131–138, Sep. 2014.

[21] J.-C. Wang, "Thermal module design and analysis of a 230 W LED illumination lamp under three incline angles," *Microelectron. J.*, vol. 45, no. 4, pp. 416–423, Apr. 2014.

[22] H. Ye, S. W. Koh, C. Yuan, H. van Zeijl, A. W. J. Gielen, S.-W. R. Lee, and G. Zhang, "Electrical–thermal–luminous–chromatic model of phosphor-converted white light-emitting diodes," *Appl. Therm. Eng*, vol. 63, no. 2, pp. 588–597, Feb. 2014.

[23] J. Wang, Y.-X. Cai, X.-J. Zhao, and C. Zhang, "Thermal design and simulation of automotive headlamps using white LEDs," *Microelectron. J.*, vol. 45, no. 2, pp. 249–255, Feb. 2014.

[24] X. Wang *et al.*, "Thermal analysis and test for convection-cooled LED lamp," (in Chinese), *J. Appl. Opt.*, vol. 35, no. 1, pp. 128–133, Jan. 2014.

[25] B. Ramos-Alvarado, B. Feng, and G. P. Peterson, "Comparison and optimization of single-phase liquid cooling devices for the heat dissipation of high-power LED arrays," *Appl. Therm. Eng.*, vol. 59, nos. 1–2, pp. 648–659, Sep. 2013.
[26] K.-S. Yang, C.-H. Chung, C.-W. Tu, C.-C. Wong, T.-Y. Yang, and M.-T. Lee, "Thermal spreading resistance characteristics of a high power light emitting diode module," *Appl. Therm. Eng.*, vol. 70, no. 1, pp. 361–368, 2014.
[27] D. Liu, H. Yang, and P. Yang, "Experimental and numerical approach on junction temperature of high-power LED," *Microelectron. Rel.*, vol. 54, no. 5, pp. 926–931, May 2014.
[28] J. Jakovenko, R. Werkhoven, J. Formánek, J. Kunen, P. Bolt, and P. Kulha, "Thermal simulation and validation of 8W LED lamp," in *Proc. EuroSimE*, Linz, Austria, Apr. 2011, pp. 1/4–4/4.
[29] D. G. Yang, H. L. Jia, and M. Cai, "Multi-physics coupling simulation of LED bulbs under temperature and humidity environment," (in Chinese), *J. Syst. Simul.*, vol. 26, no. 7, pp. 1583–1588, Jul. 2014.
[30] M. Yurtseven, S. Onaygil, and G. Ogus, "Thermal simulation and validation of LED-based luminaires using two-resistor compact thermal model," *Lighting Res. Technol.*, vol. 46, no. 5, pp. 576–586, Oct. 2014.
[31] S. Müller, T. Zahner, F. Singer, G. Schrag, and G. Wachutka, "Evaluation of thermal transient characterization methodologies for high-power LED applications," *Microelectron. J.*, vol. 44, no. 11, pp. 1005–1010, Nov. 2013.
[32] H. Chen, S. Lin, and C. Xiong, "Analysis and modeling of thermal effect and optical characteristic of LED systems with parallel plate-fin heatsink," *IEEE Photon. J*, vol. 9, no. 2, Apr. 2017, Art. no. 8200411.
[33] Y. Hsu, C.-H. Wang, and W.-F. Wu, "Lifetime distribution and reliability analysis of high-power LED assembly of street light under thermal environments," *Int. J. Rel., Qual. Saf. Eng.*, vol. 25, no. 4, Mar. 2018, Art. no. 1850017.
[34] A. Poppe, "Simulation of LED based luminaires by using multi-domain compact models of LEDs and compact thermal models of their thermal environment," *Microelectron. Rel.*, vol. 72, pp. 65–74, May 2017.
[35] A. Poppe, J. Hegedüs, A. Szalai, R. Bornoff, and J. Dyson, "Creating multi-port thermal network models of LED luminaires for application in system level multi-domain simulation using spice-like solvers," presented at the 32nd IEEE SEMI-THERM Symp., San Jose, CA, USA. [Online]. Available: https://ieeexplore.ieee.org/document/7458444
[36] M. Rencz, V. Székely, A. Poppe, K. Torki, and B. Courtois, "Electro-thermal simulation for the prediction of chip operation within the package," presented at the 19th IEEE SEMI-THERM Symp., San Jose, CA, USA. [Online]. Available: https://ieeexplore.ieee.org/document/1194357
[37] A. Poppe, O. Farkas, L. Gaál, G. Hantos, J. Hegedüs, and M. Rencz, "Multi-domain modelling of LEDs for supporting virtual prototyping of luminaires," *Energies*, vol. 12, no. 10, p. 1909, May 2019.
[38] D. Schweitzer, "Thermal transient characterization of semiconductor devices with multiple heat sources—Fundamentals for a new thermal standard," presented at the 19th THERMINIC, Berlin, Germany. [Online]. Available: https://ieeexplore.ieee.org/document/6675248?arnumber=6675248
[39] H. H. Cheng, D.-S. Huang, and M.-T. Lin, "Heat dissipation design and analysis of high power LED array using the finite element method," *Microelectron. Rel.*, vol. 52, no. 5, pp. 905–911, May 2012.
[40] Z. M. Wan, J. Liu, K. L. Su, X. H. Hu, and S. S. M, "Flow and heat transfer in porous micro heat sink for thermal management of high power LEDs," *Microelectron. J.*, vol. 42, no. 5, pp. 632–637, May 2011.
[41] J. S. Huang, T. C. Lee, and R. Tsai, "A study of heat-sink geometry on the heat transfer performance of high-power LED modules," (in Chinese), *J. Adv. Eng.*, vol. 4, no. 1, pp. 89–96, Jan. 2009.
[42] G. Barakos, E. Mitsoulis, and D. Assimacopoulos, "Natural convection flow in a square cavity revisited: Laminar and turbulent models with wall functions," *Int. J. Numer. Methods Fluids*, vol. 18, no. 7, pp. 695–719, Apr. 1994.
[43] *Transient Dual Interface Test Method for the Measurement of the Thermal Resistance Junction-to-Case of Semiconductor Devices With Heat Flow Through a Single Path*, Standard JEDEC JESD51-14, 2010.
[44] C. J. M. Lasance and A. Poppe, *Thermal Management for LED Applications: Thermal Testing of LEDs* (Solid State Lighting Technology & Application Series), vol. 2. New York, NY, USA: Springer, 2014, pp. 73–165. [Online]. Available: https://link.springer.com/chapter/10.1007/978-1-4614-5091-7_4
[45] M. Cai, D. Yang, K. Tian, P. Zhang, X. Chen, L. Liu, and G. Zhang, "Step-stress accelerated testing of high-power LED lamps based on subsystem isolation method," *Microelectron. Rel.*, vol. 55, pp. 1784–1789, Aug./Sep. 2015.

MIAO CAI received the M.S. and Ph.D. degrees from the Guilin University of Electronic Technology (GUET), China, in 2009 and 2017, respectively. Since July 2008, he has been with Flextronics International Corporation, Zhuhai, China, worked on reliability testing and failure analysis of electronic products, for three years. Since July 2011, he has been with the Research Center of Microelectronics Packaging Technology, GUET. His research interests include LED packaging and system integration, SMT-SREKs design and manufacturing, and reliability analysis.

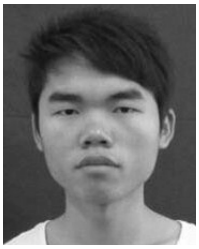

ZHI LIANG received the bachelor's degree from the Guilin University of Electronic Technology (GUET), China, in 2017. Since September 2017, he has been with the Research Center of Microelectronics Packaging Technology, GUET. His research interests include LED packaging and reliability analysis.

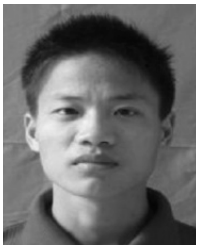

KUN-MIAO TIAN received the bachelor's degree from the Guilin University of Electronic Technology (GUET), China, in 2015. Since 2015, he has been with Guilin Changhai Development Company Ltd., Guilin, China, worked on automatic controlling and failure analysis of electronic products, for four years. His research interests include LED packaging, system integration, and reliability analysis.

MING-HUI YUN received the M.S. degree from the Guilin University of Electronic Technology (GUET), China, in 2016. Since 2016, he has been with Zhongxing Telecommunication Equipment Corporation (ZTE), Shenzhen, China, worked on Supply Chain and the Production Department, for two year. Since September 2018, he has been with the Research Center of Microelectronics Packaging Technology, GUET. His current research interests include advanced manufacturing technology, microsystems packaging technology, and reliability analysis.

PING ZHANG received the M.S. degree from the Guilin University of Electronic Technology (GUET), China, in 2007, and the Ph.D. degree from the Nanjing University of Science and Technology (NUST), in 2009. Since July 2013, he has been an Associate Professor with the School of Mechanical and Electrical Engineering, GUET. His research interests include heat transfer at contact interface, thermal management for electronics, and microelectronics reliability.

DAO-GUO YANG received the M.S. degree from Zhejiang University, China, in 1989, and the Ph.D. degree from the Delft University of Technology, The Netherlands, in 2007. He was a Postdoctoral Research Fellow with TU Delft, for two years. Afterward, he jointed Philips Semiconductors (NXP Semiconductors, The Netherlands), as a Principal Engineer and a project leader. Since 2009, he has been a Professor with the College of Mechanical and Electrical Engineering, Guilin University of Electronic Technology, China. His current research interests include microelectronics and microsystems packaging technologies, LED packaging and system integration, reliability analysis, and numerical and experimental mechanics.

GUO-QI ZHANG received the Ph.D. degree in aerospace engineering from the Delft University of Technology, Delft, The Netherlands, in 1993. He was with Philips for 20 years as Principal Scientist, from 1994 to 1996, the Technology Domain Manager, from 1996 to 2005, a Senior Director of Technology Strategy, from 2005 to 2009, and a Philips Fellow, from 2009 to 2013. He also had part time appointments as a Professor with the Technical University of Eindhoven, from 2002 to 2005, and the Chair Professor with the Delft University of Technology, from 2005 to 2013, where he has been the Chair Professor with the Department of Microelectronics, since 2013. As one of the renowned players in the fields of semiconductors and SSL technologies, he is also the Deputy Director of the European Center for Micro- and Nanoreliability (EUCEMAN), the Vice Chairman of the Chinese Electronics Packaging Association, and the China Co-Chairman of the Advisory Board of International Solid State Lighting Alliance (ISA). His current research interests include micro/nanoelectronics system integration, microsystems packaging, and assembly technologies and reliability.